atmosphere

Article

Insights on Polar Day Antarctica Radio Propagation Using Amateur Radio Beacons on Circumnavigating Balloons

Todd McKinney [1,*], Nick Perlaky [1], Mike Newchurch [1,*] and Bill Brown [2]

[1] Shelby Center for Science and Technology, The University of Alabama in Huntsville, 301 Sparkman Dr NW, Huntsville, AL 35899, USA; nick.perlaky@uah.edu
[2] NASA Marshall Space Flight Center, Martin Rd SW, Huntsville, AL 35808, USA; william.j.brown@nasa.gov
* Correspondence: tm0155@uah.edu (T.M.); mike.newchurch@uah.edu (M.N.); Tel.: +1-(803)-322-3692 (T.M.)

Abstract: We deployed six pico balloons with 20 m transmitters (14.09 MHz) from Neumayer Station III in the 2022 Antarctic summer. Our objective was to evaluate ionospheric propagation in lower latitudes. Leveraging the Weak Signal Propagation Reporter (WSPR) protocol, we transmitted and received telemetry data on a global scale. Each balloon remained airborne for over a month, with one completing eight circumnavigations of the southern hemisphere, transmitting WSPR beacon data for 98 days. Our analysis focused on signal propagation characteristics in the polar ionosphere and surrounding regions, considering factors such as location relative to the WSPR network and solar elevation angles. Alignment between solar elevation angles at transmitting and receiving stations indicated a relationship with signal reception; lower solar elevation angles proved crucial for long-range propagation. We discovered that, beyond a solar angle of 60 degrees above the horizon, no decodes were recorded beyond 7500 km. Most signal spots were observed within a 1000–5000 km range and solar elevation angles ranging from 1 to 80 degrees. Over Antarctica, spot occurrences peaked around 4 UTC, particularly during the early hours of the day. Our findings demonstrate the usefulness of pico balloons for propagation studies, providing insights into the WSPR network's coverage over Antarctica and surrounding lower latitudes.

Keywords: radio propagation; polar ionosphere; balloons; HF propagation

Citation: McKinney, T.; Perlaky, N.; Newchurch, M.; Brown, B. Insights on Polar Day Antarctica Radio Propagation Using Amateur Radio Beacons on Circumnavigating Balloons. *Atmosphere* **2023**, *14*, 1118. https://doi.org/10.3390/atmos14071118

Academic Editors: Emilia Correia, Jean-Pierre Raulin, Paulo Roberto Fagundes and José-Valentin Bageston

Received: 11 June 2023
Revised: 30 June 2023
Accepted: 3 July 2023
Published: 5 July 2023

1. Introduction

The ionosphere is a highly ionized layer of the Earth's upper atmosphere that can reflect, refract, and scatter radio waves, influencing their paths and properties. Radio propagation has served as a key method of communication and research of the ionosphere since the early 1900s [1]. Profiling ionospheric propagation involves sending radio signals from a transmitter and measuring the strength and quality of the received signals at various locations using specialized equipment such as signal analyzers or spectrum analyzers. A popular method of profiling ionospheric propagation is the WSPR (Weak Signal Propagation Reporter) protocol developed by Dr. Joe Taylor in 2008. The WSPR network encompasses a vast array of beacon transmitters and observers positioned worldwide. This network contributes to a global database (wsprnet.org), which records essential information such as the timestamp of established links between two radio stations, along with their corresponding call signs and geographical locations. WSPR rapidly gained popularity among amateur radio operators for its ability to detect very weak signals and report propagation conditions over long distances [2]. Today, WSPR is extensively utilized by amateur radio operators and researchers to study radio propagation and conduct experiments in radio communication, with applications encompassing grayline propagation [3], antenna testing and design [4], and the investigation of solar eclipse effects on radio propagation [5].

Despite the significant growth of the WSPR infrastructure in recent years, certain regions still lack operational stations, creating coverage gaps. The majority of WSPR stations are concentrated in the United States, Europe, Australia, New Zealand, and South America. Moreover, not all stations possess the capability to both transmit and receive signals. These factors, combined with the diverse equipment used by amateur radio operators operating the network, present challenges in conducting propagation studies from a single site. This is apparent when considering scenarios wherein a signal is transmitted and received by only one station within a specific area. In such cases, it becomes uncertain whether the signal's limited reception is a result of propagation characteristics or if the decoding reliability of the equipment determines the signal's apparent endpoint. Furthermore, the absence of an official record detailing the operating schedules for WSPR equipment can lead to misinterpretations, as the observed operation schedule may be misconstrued as a pattern in propagation conditions [3]. The non-uniform distribution of stations, variations in equipment, and potential misinterpretations necessitate a comprehensive understanding of these constraints to ensure accurate and meaningful analyses within the WSPR network.

Antarctica has been particularly affected by the limited WSPR coverage due to the formidable logistical challenges involved in establishing and maintaining a WSPR infrastructure in such harsh conditions. This absence of wider WSPR coverage is regrettable considering the significance of studying the ionosphere at low latitudes for both space weather and propagation investigations [6–9]. In order to address this gap, a WSPR station, known as DP0GVN, was established in 2018 at the Alfred Wegener Institute (AWI) Neumayer Station III, situated at 70.666 S, 8.2667 W [10,11]. The primary objective of this station is to acquire valuable insights into the behavior of radio wave propagation within the Antarctic ionosphere, specifically focusing on frequencies ranging from 100 kHz to 50 MHz. Additionally, a separate WSPR station, KC4USV, was set up at the American McMurdo Station (77.8500 S, 166.6667 E) in 2022 for amateur radio operations. It is worth noting that only the DP0GVN station at Neumayer has been observed to receive signals, establishing Neumayer as the exclusive permanent WSPR receiving station in Antarctica. Another WSPR station, known by the call sign DP0POL, is installed on the AWI Icebreaker Polarstern. This ship occasionally voyages to Antarctica; however, it does not consistently operate or receive data.

Initial findings from the DP0GVN station at Neumayer indicate that the majority of reported WSPR spots originate from stations in the Northern Hemisphere. Station reports under Hartje and Walter [10] found that, during the equinox, a transition zone between daylight and nighttime runs north to south, resulting in signal paths either entirely in daylight or darkness. This creates favorable conditions for long-distance communication between Europe and Antarctica for extended periods. However, during the solstice, daylight and nighttime periods misalign, limiting the availability of open signal paths to specific time windows. Hartje and Walter [10] also demonstrated that Antarctica experiences minimal radio interference, with any potential sources of interference originating from stations located outside the continent.

Other studies have shown Antarctica to be unique for propagation on a continental scale. Using high-frequency (HF) transmitter/receiver links between the McMurdo and South Pole radio stations, Liu et al. [6] have shown that the 5.1 MHz band shows a clear E-region reflection mode and is absorbed under sunlit conditions. Liu et al. [6] have suggested that these links are attainable in Antarctica under certain radio propagation conditions, although it appears to be more sporadic in nature. Ads et al. [12] have conducted a study that has evaluated propagation between the Spanish Antarctic Station (SAS) on Livingston Island and the Ebro Observatory (OE) in Spain on HF bands (2–30 MHz). They found that, for the daytime, frequencies below 10 MHz are hindered by the D-layer's absorption, making propagation impossible. However, high signal-to-noise ratio (SNR) values can be measured from 10 MHz to 17 MHz between 7:00 UTC and 11:00 UTC. From 11:00 UTC to 18:00 UTC, this range shifts from 13 MHz to 23.5 MHz. Ads et al. [12] proposed that the existence of the highly ionized F2 layer during the daytime supports this propagation behavior.

By utilizing the WSPR network for propagation studies, researchers can gain a more comprehensive understanding of regional propagation, surpassing the limitations of previous studies that relied on data from only two individual transmitting and receiving sites. This study introduces a novel approach to profile ionospheric radio propagation using pico balloons. Furthermore, known as micro super pressure balloons, pico balloons float in the lower stratosphere/upper troposphere and can remain aloft for many months. During November 2022, six pico balloons equipped with solar-powered WSPR trackers operating on the 20 m (14.09 MHz) band were launched from Neumayer Station III and remained airborne for durations ranging from 1 to 3 months. Figure 1 displays the map indicating the locations of the balloons, the Neumayer Station, and the DP0POL Icebreaker, along with the stations that received the balloon signals throughout the study period (from 16 November 2022 to 3 March 2023). Table 1 summarizes these balloon flights.

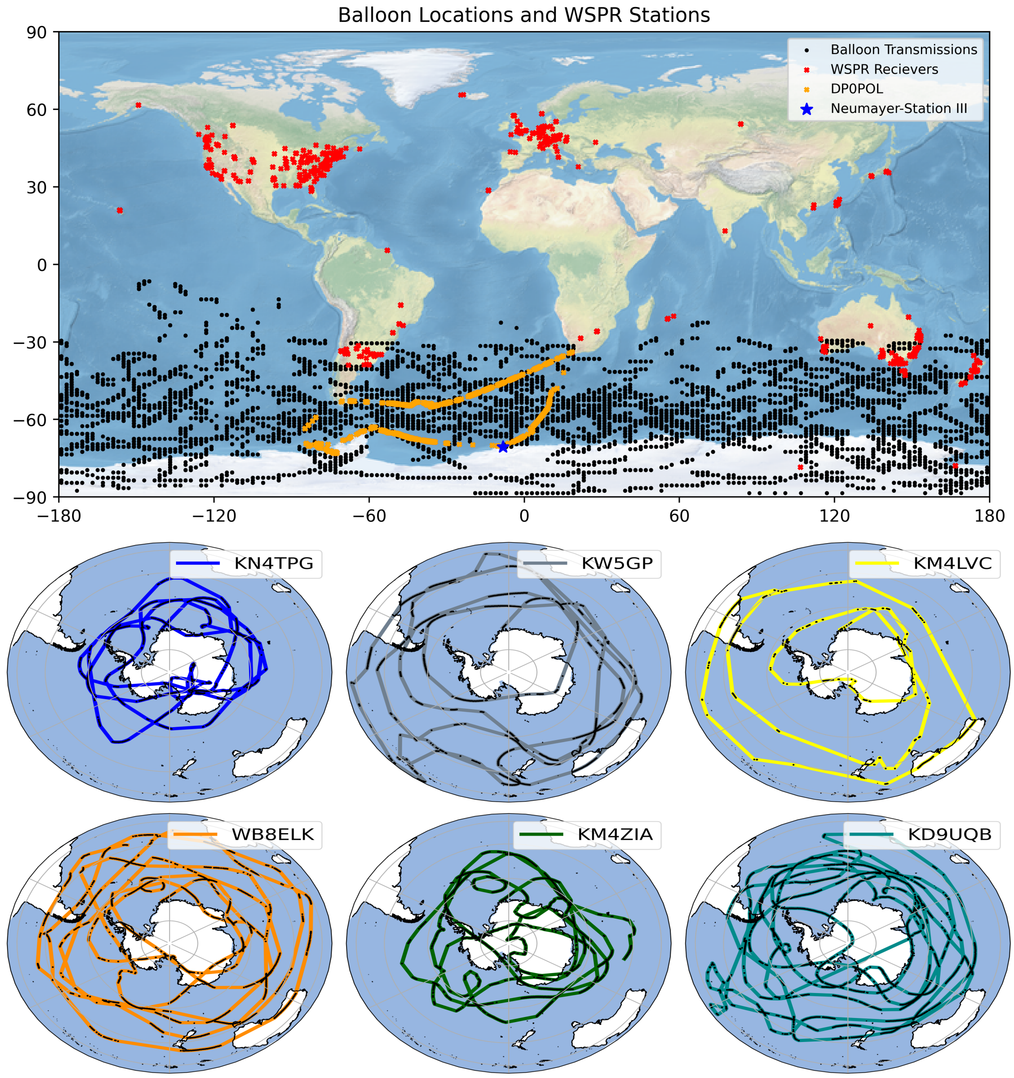

Figure 1. (**Top**) map showing the locations of the balloons during the study period, locations of the DP0POL Icebreaker, Neumayer Station, and all the WSPR stations decoding balloon telemetry throughout the study period. (**Bottom**) polar projection maps of the six balloons. Call signs for the flights are listed.

There is a rich history of using balloons for radio propagation research. Radiosonde data from weather balloon flights have been used to determine the radio refractive index of and the conditions of radio wave propagation in the atmosphere [13]. Tethered balloons have served as a telemetry link platform for remote areas, enabling access to radio links beyond the reach of ground-based systems; these balloons provide a means to establish communication over the horizon in locations that would otherwise be inaccessible [14,15].

Balloons have also been recently used to understand very low frequencies (VLFs) and their apparent frequency changes with changing altitudes [16]. While the utilization of pico balloons carrying WSPR transmitters has gained popularity among balloon and amateur radio enthusiasts in recent years [17,18], there is a lack of published literature on the propagation results obtained from these balloon flights. Utilizing balloons for propagation studies offers the advantage of comparing propagation results against specific locations, allowing for a comprehensive analysis beyond time-based observations, which is not possible with stationary WSPR setups. This approach enables us to gain insights into the coverage range of the current WSPR receiver network over Antarctica and the surrounding regions. This will be useful to determine the coverage range of a hypothetical propagation data network. For instance, weather stations on the surface could utilize WSPR instead of costly GPS modem systems to transmit data. Accurate knowledge of the range and extent of WSPR propagation over Antarctica holds significant importance for the establishment of a possible WSPR instrumentation network in the region.

Table 1. Dates and ranges for the six balloon flights.

Call Sign	Date Launched	Time Aloft (Days)	Latitude Range	Circumnavigations
KN4TPG	16 November 2022	59	87.312 S–43.229 S	5
KW5GP	16 November 2022	62	78.438 S–6.175 S	5
KM4LVC	20 November 2022	39	86.646 S–21.928 S	3
WB8ELK	20 November 2022	84	85.396 S–22.104 S	7
KM4ZIA	20 November 2022	79	88.479 S–38.688 S	6
KD9UQB	23 November 2022	98	88.770 S–13.313 S	8

Our study's results are presented in the following format. Firstly, we provide an overview of our methodology for utilizing WSPR on balloon-based platforms. Next, we discuss the raw transmissions from the balloon payloads and the stations responsible for receiving these transmissions. We then delve into the decoding capabilities of the DP0GVN station for the balloon transmissions as they circumnavigate the southern hemisphere. Lastly, we explore the properties of balloon transmissions based on solar elevation and time of day.

2. Methods

Balloon WSPR Transmitters

This study involved the deployment of WSPR trackers on pico balloons with a diameter of 0.81 m, which floated at altitudes between 10.1 and 12.5 km AMSL. Pico balloons, also known as micro super pressure balloons, are characterized by their smaller dimensions in comparison to larger stadium-sized super pressure balloons. Typically ranging from 0.5 to 2 m in diameter, pico balloons have a payload capacity of less than 50 g. The compact size of these balloons brings forth several advantages. Firstly, their small form factor allows for a larger quantity of balloons to be deployed, expanding the range of potential deployment locations. Furthermore, their reduced size contributes to lower launch and labor costs, as a single person is capable of managing each launch operation. In the context of this study, inexpensive party balloons were obtained from a party supply store and underwent pressure testing. The details regarding the testing and deployment of pico balloons will be discussed in future publications. However, it is worth mentioning that, apart from helium, all necessary equipment and materials for this study were transported to Antarctica in the carry-on luggage of a single individual. Considering the size and payload mass of these balloon flights, the required amount of lifting gas is exceptionally minimal. For instance, a typical weather balloon launch at a weather balloon station utilizes approximately 1.70 m^3 of helium, whereas a single pico balloon launch only necessitates around 0.07 m^3 of helium.

This means that 24 pico launches could be performed for the same amount of helium as a single weather balloon launch.

The WSPR transmitters utilized are depicted in Figure 2, whereas Table 2 presents the characteristics of the trackers. In this study, all WSPR payloads operated within the 20 m (14.09 MHz) band and had a payload mass below 30 g. This specific band is widely favored for WSPR operations due to its capacity to enable long-distance communication throughout both day and night, while exhibiting lower susceptibility to solar flares and other space weather disruptions compared to higher frequency bands [2]. Furthermore, due to its popularity among the amateur radio community, there is a higher probability that ham radio operators would be actively receiving and decoding telemetry data on this specific band.

Table 2. WSPR payload characteristics for each flight. Skytrackers manufactured by Bill Brown, WB8ELK, from Huntsville, AL, USA, the W5KUB Tracker made by the W5KUB group in Memphis, TN, USA, and the NIBBB tracker manufactured by the Northern Illinois Bottlecap Balloon Brigade, Chicago, IL, USA.

Call Sign	Type	Power Output (mW)	Minimum Operating Sun Angle (Degrees)	Solar Panels	Transmitter
KN4TPG	Skytracker	23.0	12.9	2× PowerFilm Solar MPT3.6-75's	Cypress CY22393FXI
KW5GP	W5KUB Tracker	10.0	15.8	1× 3.5v Polysilicon	Skyworks SI5251
KM4LVC	Skytracker	23.0	18.1	2× PowerFilm Solar MPT3.6-75's	Cypress CY22393FXI
WB8ELK	Sktracker	23.0	12.4	2× PowerFilm Solar MPT3.6-75's	Cypress CY22393FXI
KM4ZIA	Skytracker	23.0	9.2	2× PowerFilm Solar MPT4.8-150's	Cypress CY22393FXI
KD9UQB	NIBBB tracker	10.0	1.4	3× PowerFilm Solar MPT6-150	Skyworks SI5351

We utilized three different types of WSPR payloads: the SkyTracker [19], a transmitter produced by the W5KUB group [20], and a transmitter developed by the Northern Illinois Bottlecap Balloon Brigade [21]. It is worth noting that these trackers rely exclusively on solar energy to function, meaning that transmissions are not possible once the sun sets below a certain threshold. Conveniently, while close to the South Pole, some of the flights were observed to transmit 24/7 due to the polar day phenomenon. For each payload, we calculated the solar elevation angles for each balloon transmission at each location and time using the pvlib python package [22]. The lowest solar angles are listed for each individual WSPR payload in Table 2. Note that the KD9UQB payload had the lowest operating solar elevation due to the circular solar panel configuration; in addition, 3× Schottky diodes were equipped to prevent current drain from panels that were not orientated toward the Sun. The KM4LVC balloon had the highest solar elevation cut-off; we believe that this is due to potential issues with the solar panels and/or the payload's orientation, which may have affected its ability to point toward the Sun. Figure 3 shows a balloon just after launch and the balloon line schematic for each flight. The payloads are suspended with taut fishing line and the antennas are supported without tension. To maintain tension in the bottom line, a small tape ball is attached as a weight.

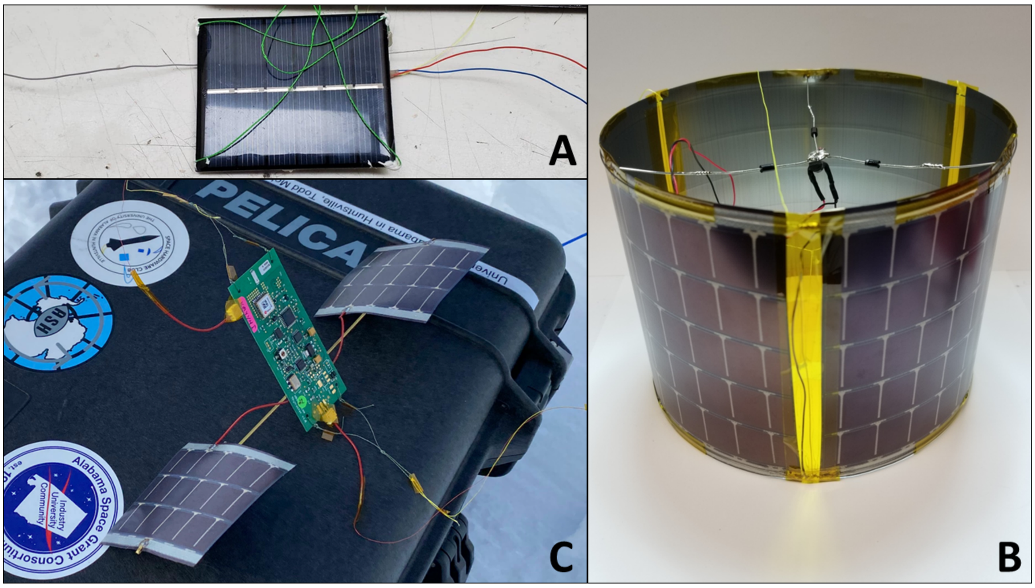

Figure 2. Depiction of the 20 m WSPR payload varieties flown in this study. (**A**) KW5GP payload built by the W5KUB group, (**B**) KD9UQB payload built by the NIBBB group, and (**C**) WB8ELK Skytracker flying the KN4TPG, KM4LVC, WB8ELK, and KM4ZIA call signs.

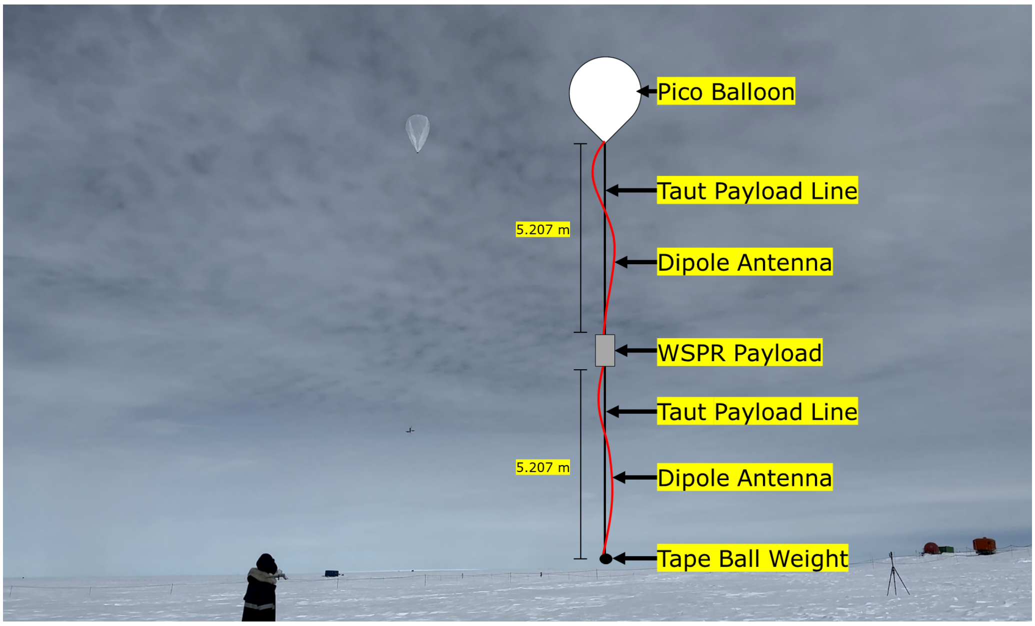

Figure 3. Balloon diagram and flight photo showing the line setup for each balloon flight. Red lines indicate antennas and black lines indicate payload lines.

The WSPR trackers work as follows: a 2 min transmission is sent out to report the balloon location in the WSPR grid square format. The size of these grid squares is approximately 1 degree of latitude by 2 degrees of longitude, which translates to roughly 6190 square kilometers at the equator. However, the actual area of the grid squares varies based on the latitude of the grid square. This can be found by

$$A = (\cos(\phi) \times 111.32)^2/2 \tag{1}$$

where A is the area of the grid square in kilometers and ϕ is the latitude. The constant 111.32 km represents the length of one degree of latitude on the Earth's surface, and is derived from the circumference of the Earth.

Balloon GPS positions are reported as the center of the WSPR grid square; conveniently for this study, this means that there is a increased precision in the location as the balloons approach the poles. As an illustration, at 88 degrees south, the area of a WSPR grid square is approximately 7.5 square kilometers, significantly smaller compared to the 6190 square kilometers at the equator.

After the balloon transmission, if the signal is heard by a surface WSPR station, the station will decode and upload the report to the central database located on wsprnet.org. On this website, the following variables are logged: report ID, UTC time of report, frequency of the report, call sign of the receiver, receiver's latitude and longitude, the call sign of the transmitter (in this case, the balloon call sign), transmitter's latitude and longitude, the distance and azimuth between the transmitter and receiver, and the SNR of the signal. Although we set our balloon transmitters to send a second 8 min transmission to improve location resolution and provide additional information about the balloon flight, these transmissions will not be utilized in this propagation study. This is because they use a telemetry call format instead of a location grid-square format, which makes them irrelevant for the specific objectives of this study.

One of the unique aspects of flying a transmitter is its ability to have a longer line of sight range to the horizon. This aspect can be demonstrated by

$$d = \sqrt{h(2R + h)} \tag{2}$$

where d is the distance to the horizon, h is the height of the balloon above sea level, and R is the radius of the earth.

By plugging in the range of floating point numbers between 10 and 12.5 km, we can derive values of d equal to 357 and 399 km, respectively. It is noteworthy that these distances are significantly greater than the range of a station at sea level, which is approximately 4.7 km. There are two primary benefits to operating a transmitter at an elevated position. Firstly, it mitigates the absorption effects that a surface-level transmitter would normally encounter. When transmitting from the surface, ground clutter can attenuate the signal strength. Secondly, an elevated transmitter has a broader field of view, encompassing a greater expanse of sky from the horizon to the zenith. This is particularly advantageous when utilizing lower solar elevations for propagation, as a balloon can have access to the day–night terminator for an extended period due to the Sun setting at varying times based on altitude.

In addition to our transmitters, DP0GVN at Neumayer Station III, both transmit and receive on WSPR bands [10,11]. This WSPR station is expected to operate an entire sunspot cycle, lasting 11 years and concluding in 2030. During the study period, DP0GVN was able to detect balloon transitions for a significant portion of the time, as depicted in Figure 4; Figure 4 shows the histograms of the balloon transmissions and the latitudes of the stations uploading the transmissions to the WSPR network. This study will only focus on discussing the propagation outcomes on the 14.09 MHz band that corresponds to the balloon transmissions. Although the WSPR station at Neumayer both transmits and receives, for the scope of this study we will only be looking at the station in terms of decoding balloon transmissions. Note that the DP0POL Icebreaker, operated by AWI, Bremerhaven, Germany, is shown to be at different latitudes; this corresponds to the Icebreaker moving to different locations throughout the study period.

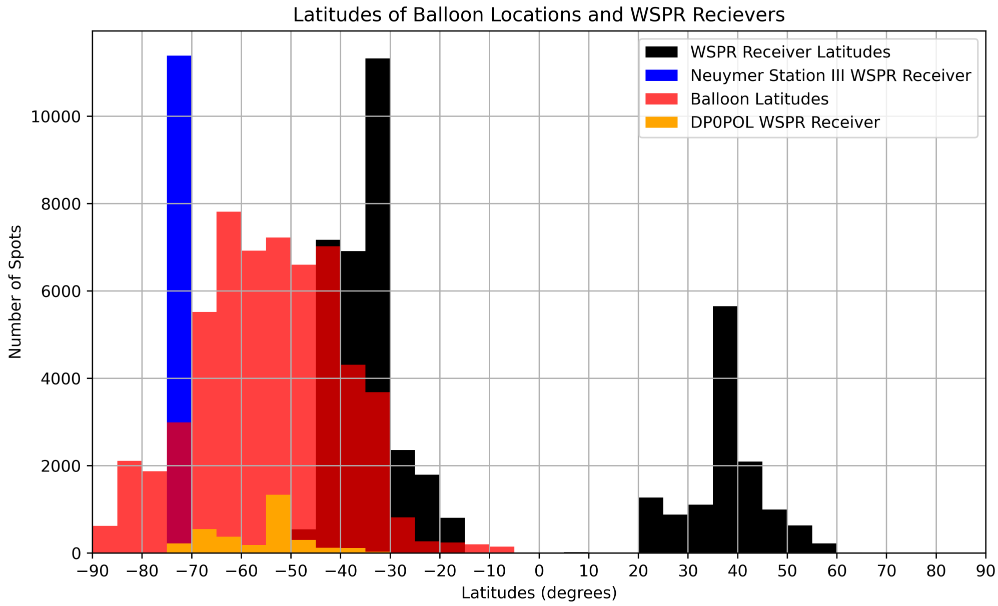

Figure 4. Histograms showing frequency of balloons latitudes in red and latitudes of WSPR stations receiving balloon telemetry. The red bars have a transparent quality that allows the bars underneath to be visible. Blue and orange show AWI WSPR receivers receiving balloon WSPR transmissions, while black shows the rest of the WSPR receiving network.

3. Results

3.1. Raw Balloon Transmissions

In this section, we will be discussing the raw transmissions from each WSPR payload. Table 3 displays WSPR averages and Figure 5 shows balloon locations of all the flights colored by signal travel distance and signal SNR. The longest flight lasted 98 days and completed eight full circumnavigations around the southern hemisphere. It is worth noting that the maximum signal distance for each WSPR exceeded 19,000 km, which is remarkable considering the small size and transmit power of each WSPR balloon tracker. To put this into perspective, the great circle distance from the South Pole to the North Pole is approximately 20,014 km. In fact, some signals from the WSPR balloon trackers even exceeded the distances achieved by nearby surface WSPR stations that transmit at powers three orders of magnitude higher than the balloons, adding to the impressive nature of this accomplishment. We see on Figure 5 that there is a correlation between the SNR and the location of the balloons, which can be attributed to the positioning of the WSPR network. For instance, the presence of good WSPR reception at Neumayer Station and various networks across Australia leads to higher SNR values (more red on right Figure 5) when the balloons are in proximity to these regions. Consequently, short-propagation higher-SNR transmissions are more likely to be received.

Table 3. WSPR spot characteristics for the six balloon flights.

Call Sign	Number of Spots	Mean SNR	Mean Distance (km)	Max Distance (km)
KN4TPG	5024	−19.3	5037	19,030
KW5GP	7050	−17.0	3224	19,570
KM4LVC	1994	−16.4	2770	19,608
WB8ELK	11,165	−18.8	4177	19,930
KM4ZIA	12,985	−17.3	5808	19,837
KD9UQ	20,137	−18.9	6188	19,879

Note: SNR stands for Signal-to-Noise Ratio.

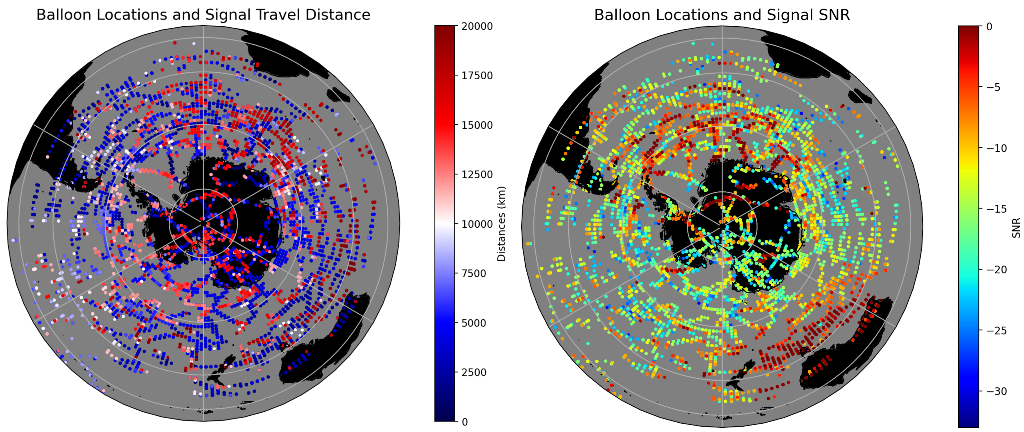

Figure 5. Balloon signal travel distances and SNR values for each balloon location. For each WSPR grid square, the farthest signal distance and highest SNRs are colored. In comparison, a 10,000 km distance is approximately from the South Pole to the equator (colored in white for the left figure), and 20,000 km is the distance from the North Pole to the South Pole, colored in dark red.

In Figure 6, each balloon flight is represented by a "Spot 2D-Histogram" showing the time aloft on the x-axis and time of day on the y-axis, which is a commonly used visualization method for analyzing WSPR spots over the course of a day. However, due to the changing location of the balloons during the flights, there are variations in solar elevation angles over time, necessitating the use of solar elevation angles rather than standard UTC time to determine the time of day, which will be further discussed in upcoming sections. This plot also highlights that payloads equipped with larger solar panels, such as the KM4ZIA and KD9UQB payloads, exhibited a higher number of transmissions throughout the flight; these payloads could transmit when the Sun was lower on the horizon.

We present box plots in Figure 7 that illustrate the distribution of WSPR transmissions across latitude and longitude coordinates of receiving stations, as influenced by the latitudes and longitudes of the balloons. We include markers for major cities and their corresponding latitude–longitude positions as a reference. This plot is immensely valuable for assessing the extent of WSPR coverage in the southern hemisphere and the surrounding Antarctic regions. By evaluating which latitude and longitude lines lie in the interquartile range, one can understand what areas receive spots based on the balloon locations. For instance, when the balloons were below the 80 S latitude (directly over the Antarctica continent), Neumayer Station was responsible for almost half (48 percent) of the balloon spot reports. This is shown by the left top plot which has the latitude line of Neumayer Station between the minimum, the lower quartile range, and the median of the box plots below the 80 S latitude. This finding highlights the significance of the DP0GVN station for WSPR propagation in Antarctica and the surrounding low latitudes.

We also have seen that more signals where decoded between 50 S and 20 S in the southern hemisphere than in the northern hemisphere between latitudes 20 N and 60 N. This is different than the findings by Hartje and Walter [10] which reported more decodes from the northern hemisphere. This demonstrates the benefits of balloon-based WSPR beacons; the balloons were able to travel to locations that had more WSPR coverage in the southern hemisphere. The majority of signal decodes between longitudes 100 E and 170 E originate from stations in Australia and New Zealand. This region is the area for which the DP0GVN station had the most trouble making decodes from balloon transmissions. The addition of a WSPR receiver in Antarctica somewhere between the longitudes 179 W and 100 W may greatly improve the coverage. South America demonstrated WSPR coverage, primarily within the range of 80 W–40 W longitudes. However, the decoding of signals from more distant transmissions proved less efficient for the South American network, relying heavily on balloons in closer proximity or directly over the continent. This observation leads us to conclude that the quality of radio and antenna equipment in the WSPR stations within this region may be a contributing factor. Similar to South America, India and China also faced similar challenges in terms of WSPR signal decoding; while there were occasional decodes, they were infrequent unless the balloons were in very close proximity to these regions. However, in the case of India and China, no balloons traveled to the far northern latitudes, resulting in sporadic and long-distance signal spots. Both countries may greatly benefit from improved radio equipment for conducting radio studies in the region. Although signals were received in the United States, Europe, and Japan, decodes were more sporadic and happened less frequently simply due to the large distances between the balloons and the receivers. If the balloons had more transmit power, such as the 5000 mW power that many surface stations operate with, it is more likely that these stations would have been reached just like the DP0GVN spots, as reported by Hartje and Walter [10].

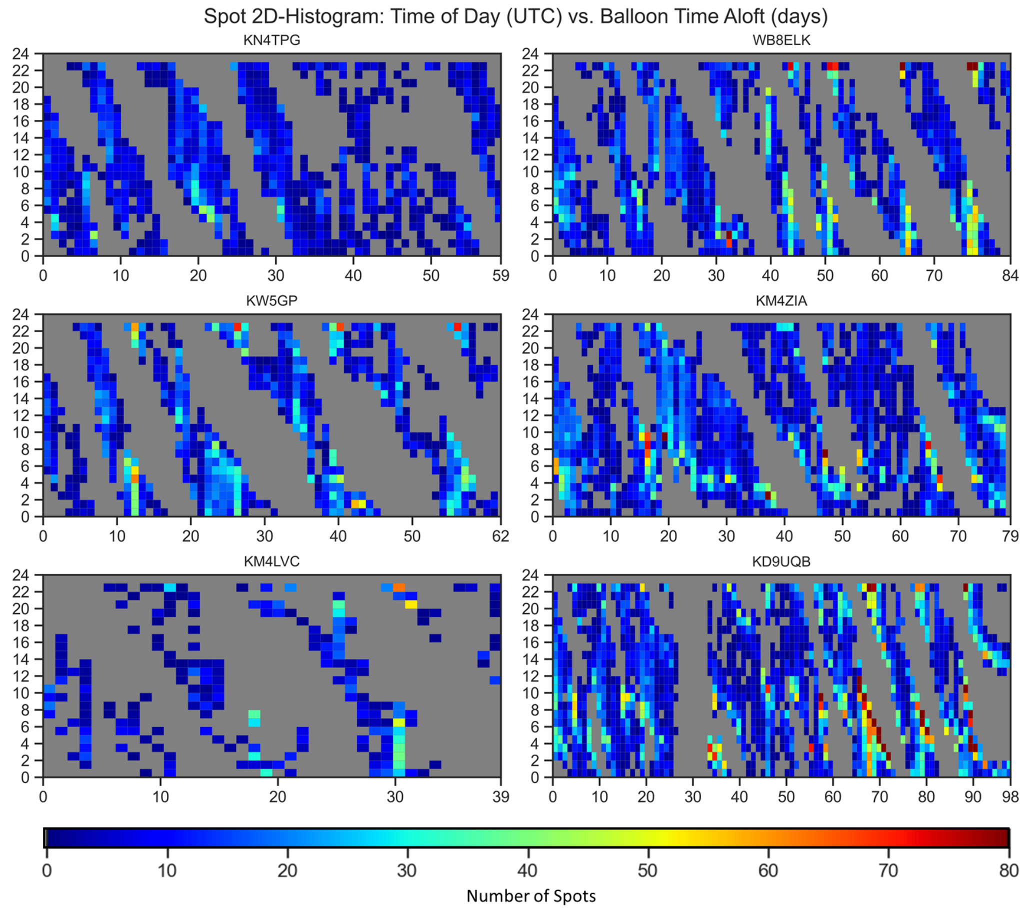

Figure 6. Spot 2D-Histogram for each individual balloon payload.

3.2. DP0GVN Decoding Balloon Transmissions

The DP0GVN station proved to be a crucial asset for WSPR operations in the southern hemisphere region. In this section, we focused on filtering spot reports from the WSPR database to specifically include balloon transmissions received by the DP0GVN station. Throughout the study period, DP0GVN had three distinct receiving channels: DP0GVN, DP0GVN/1, and DP0GVN/3. The received packets were uploaded to wsprnet.org under these call signs. Figure 8 presents SNR box plots categorized by distance. It was observed that, at the time of launch, the DP0GVN stations exhibited the highest SNR values. This was due to the tracker being within the line of sight of the WSPR receiver, resulting in an average SNR of 5. However, as the balloon moved approximately 400 km away from the station and went over the horizon, the mean SNR values dropped to −10. With increasing distance from the station, the mean SNR values gradually decreased to −20. Notably, between distances of 1200 km and 4000 km, the data exhibited a significant number of outliers in SNR values. Some packets in this range displayed strong signal returns with an SNR of 10. The presence of these outliers suggests that there were instances wherein the SNR deviated significantly from the expected trend. Various factors can contribute to these outliers, including ionospheric conditions, multipath propagation, and path loss or gain due to atmospheric conditions. Further investigation and analysis of these outliers may be necessary to determine the specific causes behind their occurrence. It is noteworthy that these outliers are more likely to happen at lower solar elevation angles; we further discuss this in the next section.

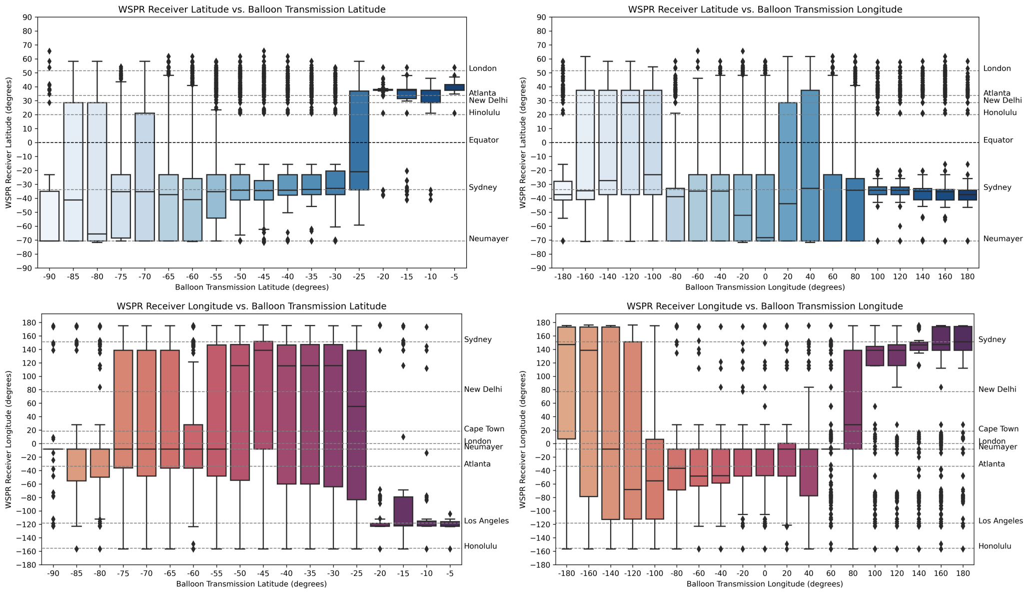

Figure 7. Box plot showing WSPR receiving latitudes and longitudes vs. balloon transmitters latitudes and longitudes. Major cities and their latitudes and longitudes are listed for location reference. Blue color scale represents WSPR receiver latitudes as function of balloon locations, with lighter colors signifying lower latitudes. For longitudes, bins get darker moving west to east. Red color scale represents WSPR receiver longitudes as function of balloon locations, with lighter colors signifying lower latitudes. For longitudes, bins get darker moving west to east. Diamonds represent outliers in the spot data set.

In addition to box plots, we present polar bar plots in Figure 9 showing SNR and azimuths of the signals relative to the receiving station. Bars are colored by the SNR values. On the left plot we show the full WSPR network and on the right we show the DP0GVN station. For the full WSPR network, we see that the majority of the spots are from the south. Spots rarely come from the north, as most of the receiving stations are at higher latitudes, and mostly occurred when the balloons were directly over a WSPR station. This is also interesting in that signals were most likely to be decoded when directly south of the WSPR stations directly on a constant longitude line. The polar plot on the right displays the receiving spots exclusively from the DP0GVN station throughout the study period. The majority of balloon decodes were received from the east direction. The highest SNR values were observed from the northwest–west region. On the other hand, the lowest SNR value decodes were received from the southeast–southwest region. A notable observation in the DP0GVN WSPR receiving network is the significant gap between the south and west directions relative to the station. This area was previously discussed in the preceding section, wherein balloons were positioned on the opposite side of the continent and establishing communication with stations in New Zealand and Australia. Compared to box plots, these regions typically had SNR values at -20. For this study, balloon transmissions were only decoded by DP0GVN when the balloon's distance was less than 8400 km.

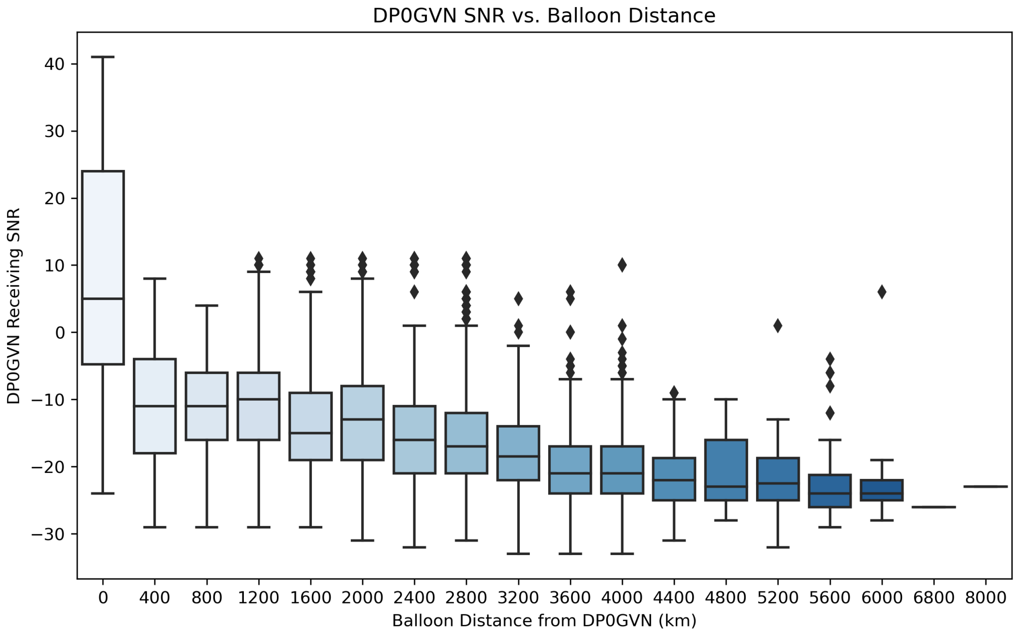

Figure 8. SNR vs. distance box plots for the DP0GVN station decoding balloon transmissions. Blue color scale is used, where darker bins represent farther distances from the DP0GVN station. Diamonds represent outliers.

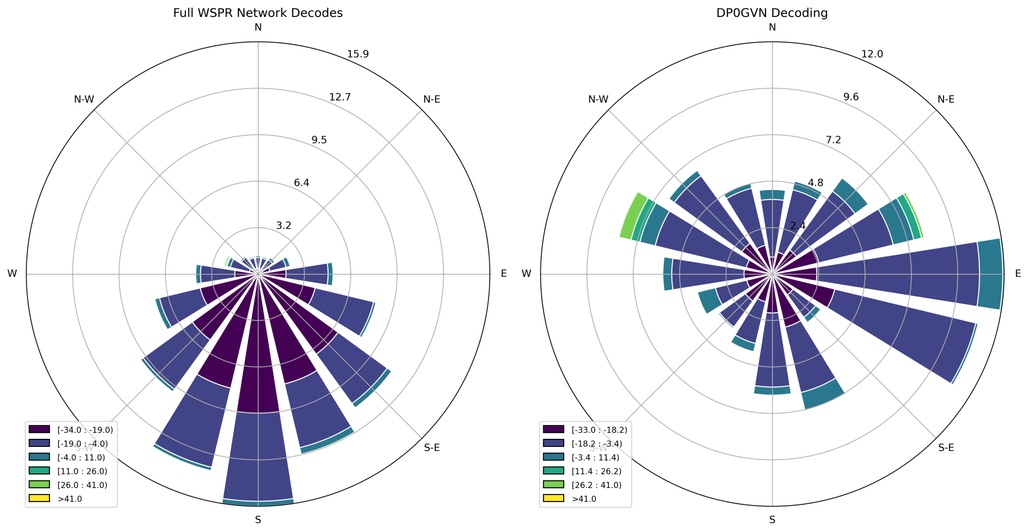

Figure 9. Frequency rose showing the directions and SNRs for the full WSPR network decoding balloon telemetry (**left**) and the DP0GVN station (**right**). Azimuths are relative to the receiving station. SNR ranges colored in the legend. The radius values are the percentages of the spot occurrences (i.e., out of the dataset, what percentage of the spots was heard from that direction).

3.3. Effects of Time of Day and Solar Elevation

For this study, the constantly changing latitude and longitude of the balloons pose a challenge in associating UTC time and solar angles over a few days. Figure 10 presents histograms depicting the number of spots based on solar elevation and hour of day (UTC), categorized by balloon latitude. Notably, higher latitude ranges have larger solar elevation bins. In this figure, observations over Antarctic regions (90 S to 70 S) reveal solar angles ranging from 0 to 42 degrees. The occurrence of spots in the WSPR data aligns with a peak around 4 UTC, similar to Hartje and Walter's [10] findings indicating a significant proportion of transmissions between 21 and 4 UTC from the DP0GVN station. The hypothesis by Ads et al. [12] of a highly ionized F2 layer over Antarctica during polar day supports this spot peak, although there is a slight discrepancy in the optimal performance time between the studies, possibly due to methodological differences in capturing propagation characteristics at specific stations versus the comprehensive coverage of the WSPR ground network in our study.

At latitudes other than the Antarctic region, we observe higher solar elevation angles spanning from 0 to 80 degrees. We see that, within the latitude range of 40 S–10 S, there is a distinct peak wherein more signals were sent when the solar elevation was between 20 and 40 degrees. Among the three latitude ranges analyzed, we observe that the decrease in spots with the progression of hours is less sudden for lower latitudes (90 S to 70 S) compared to latitudes between 70 S and 30 S. This could be attributed to the less distinct boundary between darkness and daylight caused by the Sun's low position in the polar sky. An article in Electronic [23] states that stations situated at dawn experience an increase in Maximum Usable Frequency (MUF), while those at dusk encounter a decline. The same article states that grayline-type enhancements can even affect higher-frequency signals. Recent research by Lo et al. [3] has demonstrated the prevalence of grayline propagation between the United Kingdom (UK) and New Zealand, where sunset and sunrise times play a significant role. Particularly, Lo et al.'s [3] study observed that 7 MHz WSPR communication links from the UK to New Zealand predominantly occurred during sunset, while links from New Zealand to the UK mainly took place during UK sunrise hours. Although the frequency used in our study is 14 MHz, which is double the frequency used in Lo's research (7 MHz), it is plausible that the higher polar day ionosphere is more vulnerable to ionospheric disturbances in the D region, thereby increasing the chances of lower elevation propagation.

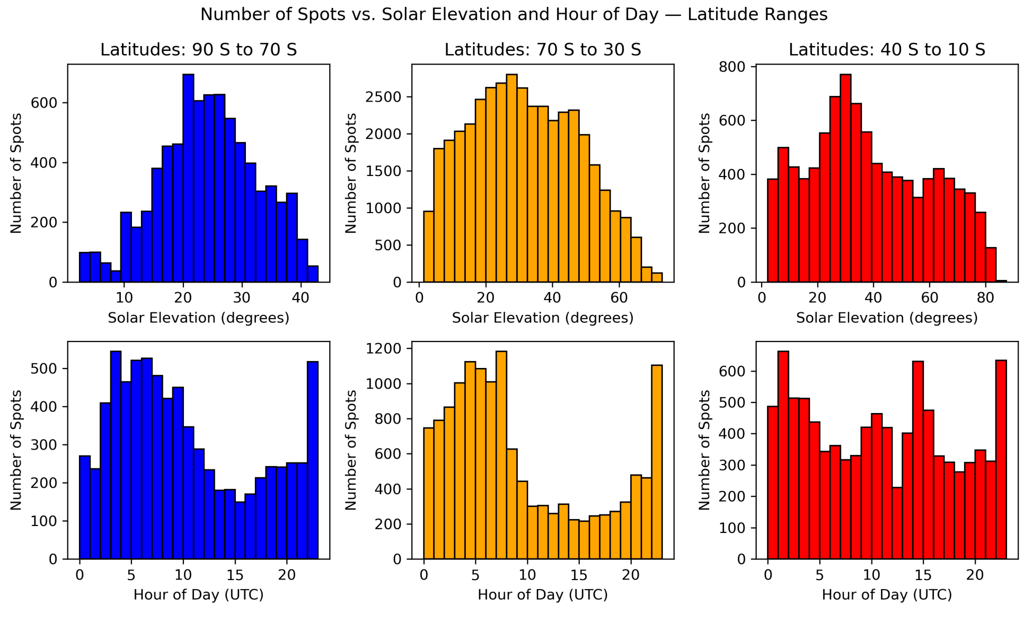

Figure 10. Histograms showing frequency of spots based on solar elevation and hour of the day (UTC). From left to right, date set is parsed by latitude ranges of the balloons.

Figure 11 shows another "Spot-2D" histogram, this time plotting signal travel distance on the x-axis and solar elevation of the transmission location on the y-axis. The data presented in this plot highlight an interesting pattern regarding balloon transmissions during the study period. It reveals that no decodes were recorded beyond a distance of 7500 km when the solar angle reached 60 degrees above the horizon. It is worth noting that the balloon trackers relied on solar power, and as a result, transmissions were not made when the solar elevation angles fell below the specified values outlined in Table 2. The majority of signal spots were concentrated within the distance range of 1000–5000 km, accompanied by a varied range of solar elevation angles at the time of transmission, spanning from 1 to 80 degrees. In Figure 11, it is notable that there is a decrease in the number of spots between a signal travel distance of 400 km and 1500 km. We hypothesize that this region corresponds to the skip zone, where signals propagate over WSPR receiving stations, resulting in fewer spots being registered. Above a signal travel distance of 1600 km, we believe that this range represents the optimal distance for a single skip in propagation. Interestingly, the central tendency of the distribution occurs at approximately 30 degrees of solar elevation and a signal travel distance of 1750 km, which we consider the most likely conditions for short-hop propagation during the study period for the 20 m band. Additionally, another distribution was observed below the 1000 km mark, specifically ranging between 30 and 40 degrees of solar elevation angle. These decodes represent line-of-sight transmissions, occurring within shorter distances from 0 to 399 km. This distribution indicates instances when the balloons were directly within the field of view of WSPR stations. Such occurrences were more likely in areas with denser WSPR networks, including shortly after launch at Neumayer, while flying over Australia, New Zealand, or South America.

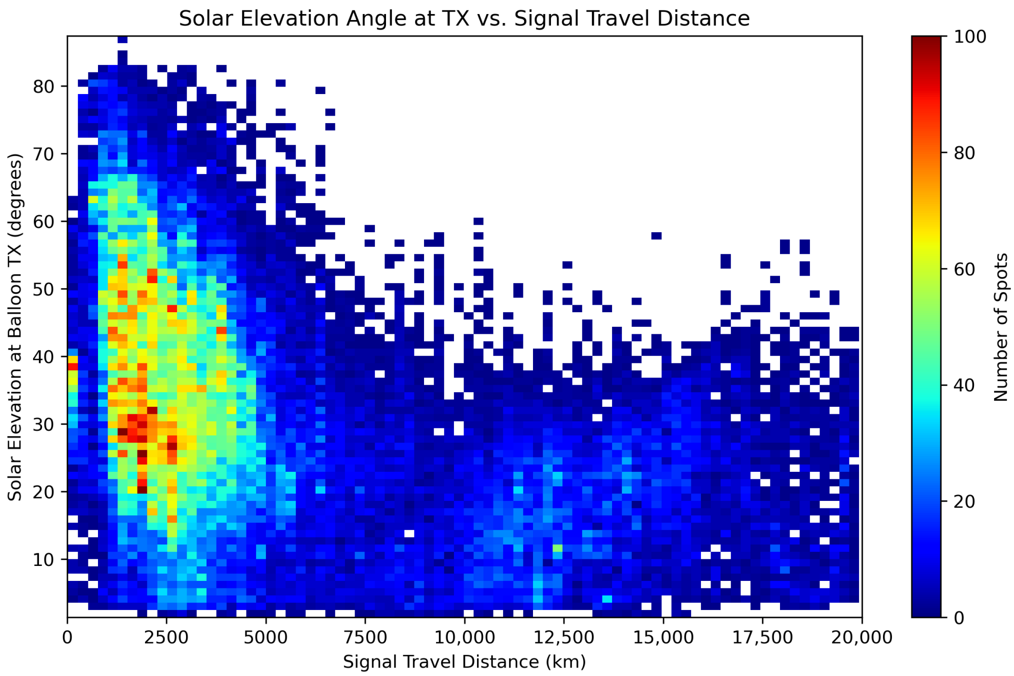

Figure 11. Spot 2D-Histogram of solar elevations during balloon transmissions vs. signal travel distance.

To further assess radio propagation influenced by solar elevation angles, we present a method that involves comparing the solar elevation angle at the transmitting (TX) station to the solar elevation angle at the receiving (RX) station. In Figure 12, we present another 2D-histogram plot where the RX solar elevation of the balloon is plotted on the x-axis, and the TX solar elevation of the receiving station is plotted on the y-axis. Additionally, we include a 1-to-1 line on the plot for reference. The presence of the 1-to-1 line in this plot serves as a valuable tool for evaluating whether the solar elevation at the TX location matches that at the RX location. By analyzing the correlation between solar elevations at different points along the transmission path, the 1-to-1 line provides insights into instances of day–night terminator propagation or when the balloon and RX station are in close proximity. Between RX solar elevation angles of 42 degrees and 90 degrees, there is a stronger alignment along the 1-to-1 line, with a tendency toward higher RX angles. This indicates that signals transmitted at lower solar elevation angles are more likely to be received by stations with higher elevation angles. To the left of this range, between 0 degrees and 42 degrees of RX solar elevation angles, there is a distribution region marked by black dotted borders. It is noteworthy that the majority of points within this region correspond to the DP0GVN decodes. These decodes are particularly interesting because they exhibit

RX solar elevation angles that never fell below 0 degrees or exceeded 45.6 degrees. This observation is attributed to the phenomenon of polar day, wherein DP0GVN experienced continuous daylight during the study period. Another intriguing finding is that the decoding of signals by receiving stations during nighttime, indicated by RX solar elevation angles below 0 degrees, was more likely to occur when the TX solar elevation angles were below 50 degrees. Consequently, RX solar elevation angles below 0 degrees did not follow the 1-to-1 line, suggesting that different propagation characteristics were at play during these instances. These findings highlight the influence of solar elevation angles on signal propagation and decoding, emphasizing the unique dynamics associated with the ionosphere at lower latitudes.

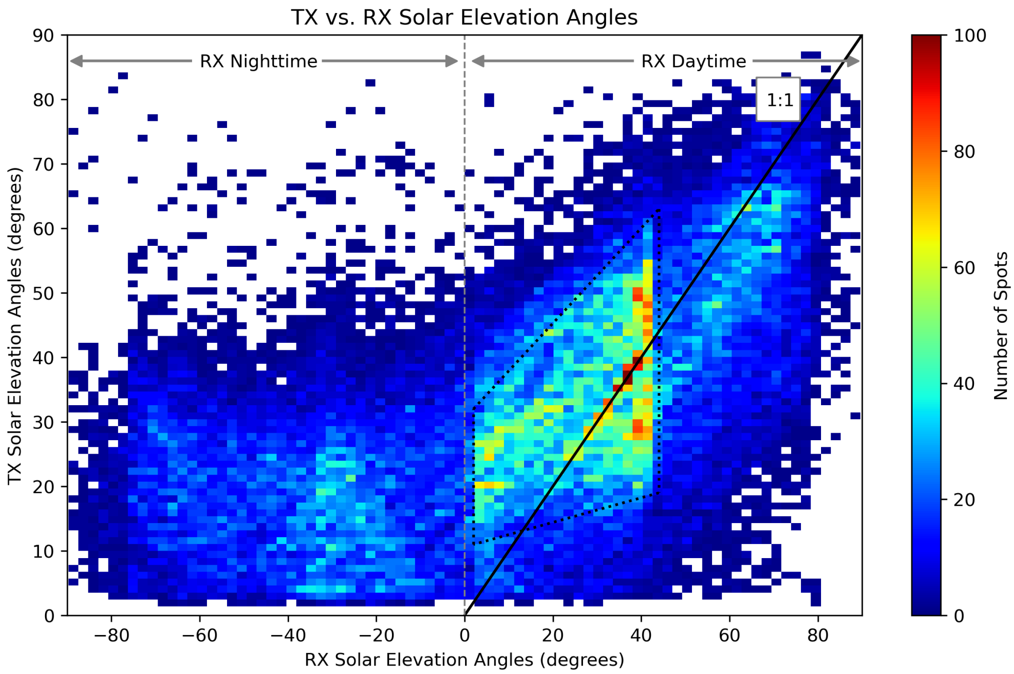

Figure 12. Spot 2D-Histogram of solar elevations during balloon transmissions vs. solar elevations of the receiving stations. A 1-to-1 line is plotted. Dotted lines indicate short hops decoded by the DP0GVN station.

4. Conclusions

Our study focused on evaluating ionosphere propagation using six pico balloons over Antarctica and at lower latitudes. Through the use of balloon-based WSPR beacons, we were able to conduct propagation studies on a broader scale compared to surface-based WSPR stations. Our findings reveal that the number of decodes is influenced by both the location of the balloons in relation to the WSPR network and solar elevation angles.

The DP0GVN station accounted for many of the balloon spots during the study period, but encountered challenges in decoding when the balloons were situated between longitudes 100 E and 179 E and between latitudes 50 S and 5 S. The Australian and New Zealand stations achieved successful WSPR decodes to fill in this gap when the balloons were in the region. The stations in South America and India faced difficulties in decoding transmissions due to lower antenna quality. In Europe, the United States and Japan signals were received, but at significantly lower spot counts compared to the southern hemisphere stations, primarily due to differences in transmission power.Our findings demonstrate that, on the 20 m (14.09 MHz) band, signal travel distances exceeding 7500 km were only observed when the solar elevation angle was below 60 degrees at signal transmission. The majority of signal spots detected during the study were concentrated within a distance range of 1000–5000 km. These spots corresponded to a wide range of solar elevation angles at the time of transmission, ranging from 1 to 80 degrees. We have also shown that a decease in spots going into the day is less abrupt for lower latitudes (90 S to 70 S) compared to latitudes between 70 S and 30 S, likely due to the less distinct boundary between darkness and daylight.

In future studies, it may be beneficial to deploy balloons equipped with WSPR transmitters operating on various frequency bands. For example, the simultaneous deployment of three balloons with transmitters on the 40 m band (7 MHz), 20 m band (14 MHz), and the 10 m band (28 MHz). This could provide insights into the characteristics of different bands, especially in scenarios wherein specific frequency ranges may be more suitable due to factors such as interference, noise, or ionospheric conditions.

The utilization of pico balloons carrying these transmitters proved to be remarkably valuable, especially considering their affordability, with each flight costing approximately $200. The authors anticipate that pico balloons will become more prevalent in research settings for radio and atmospheric science applications. Additionally, they hope that the publicly available data from this study, accessible on wsprnet.org, will be further explored by other researchers.

Author Contributions: Conceptualization, T.M. and B.B.; methodology, T.M.; software, T.M. and B.B.; resources, M.N. and N.P.; data curation, T.M.; writing—original draft preparation, T.M.; writing—review and editing, M.N. and N.P. All authors have read and agreed to the published version of the manuscript.

Funding: This research was funded by the University of Alabama in Huntsville's Collage of Science, the Earth System Science Center, and the University of Alabama in Huntsville's Atmospheric and Earth Science Department. Station time was awarded by the Alfred Wegener Institute under proposal number NM-S-AWI00-ASH.

Data Availability Statement: All data is available and archived at wsprnet.org (accessed on 29 March 2023) under call signs listed in this publication.

Acknowledgments: We would like to extend our deepest gratitude to Neumayer Station III for their exceptional hospitality, as well as express our heartfelt thanks to Markus Schulze for their invaluable assistance with balloon launches and logistics. Our sincere appreciation goes to the University of Alabama in Huntsville's College of Science, and the Earth System Science Center for their generous funding. We would also like to acknowledge the contributions of Tom Medilin and the W5KUB group, Jim Janiak with the Northern Illinois Bottlecap Balloon Brigade, and Michael Seedman for their valuable contributions to the balloon trackers. Lastly, we are profoundly grateful to the HYSPLIT team at NOAA Air Resources Laboratory for their unwavering support.

Conflicts of Interest: The authors declare no conflict of interest.

Abbreviations

WSPR	Weak Signal Propagation Reporter
AWI	Alfred Wegener Institute
SNR	Signal-to-Noise Radio
TX	Transmit
RX	Receive

References

1. Hansen, P. Developments in high power longwave radio: A brief history. In Proceedings of the 2016 IEEE International Symposium on Antennas and Propagation (APSURSI), Fajardo, PR, USA, 26 June–1 July 2016; pp. 1013–1014.
2. Taylor, J. *FT8 and WSPR: Using Weak Signal Communication Digital Modes for Amateur Radio*; The National Association for Amateur Radio (ARRL): Newington, CT, USA, 2018.
3. Lo, S.; Rankov, N.; Mitchell, C.; Witvliet, B.A.; Jayawardena, T.P.; Bust, G.; Liles, W.; Griffiths, G. A systematic study of 7 MHz greyline propagation using amateur radio beacon signals. *Atmosphere* **2022**, *13*, 1340. [CrossRef]
4. Vanhamel, J.; Machiels, W.; Lamy, H. Research Article Using the WSPR Mode for Antenna Performance Evaluation and Propagation Assessment on the 160-m Band. *Int. J. Antennas Propag.* **2022**, *2022*, 4809313. [CrossRef]
5. Fry, C.D.; Rawlins, L.; Krause, L.; Suggs, R.; McTernan, J.; Adams, M.; Gallagher, D.; Anderson, S.; Allsbrooks IV, R. Effects of the 2017 solar eclipse on hf radio propagation and the d-region ionosphere: Citizen science investigation. In Proceedings of the American Geophysical Union (AGU) Fall Meeting, 2017, New Orleans, LA, USA, 11–15 December 2017.

6. Liu, B.; Perry, G.; Chartier, A. Simulating HF radio wave propagation in Antarctica between the McMurdo and South Pole stations. In Proceedings of the AGU Fall Meeting, New Orleans, LA, USA, 13–17 December 2021; Volume 2021, p. SA45C-2240.
7. Ham, Y.B.; Jee, G.; Lee, C.; Kwon, H.J.; Kim, J.H.; Zabotin, N.; Bullett, T. Observations of the polar ionosphere by the vertical incidence pulsed ionospheric radar at Jang Bogo station, Antarctica. *J. Astron. Space Sci.* **2020**, *37*, 143–156. [CrossRef]
8. Carlson H.C., Jr. The dark polar ionosphere: Progress and future challenges. *Radio Sci.* **1994**, *29*, 157–165. [CrossRef]
9. Shelley, E.; Peterson, W.; Ghielmetti, A.; Geiss, J. The polar ionosphere as a source of energetic magnetospheric plasma. *Geophys. Res. Lett.* **1982**, *9*, 941–944. [CrossRef]
10. Hartje, M.; Walter, U. 4.10 WSPR beacon—Radio beacon at Neumayer Station III for evaluation of southern hemisphere radio propagation. Expeditions to Antarctica: ANT-Land 2019/20 Neumayer Station III, Kohnen Station, Flight Operations and Field Campaigns. *Rep. Polar Mar. Res.* **2019**, *745*, 43.
11. Hartje, M.; Walter, U. WSPR RADIO beacon at Neumayer Station III for evaluation of southern hemisphere radio propagation. *Rep. Polar Mar. Res.* **2020**, *42*, 42–104.
12. Ads, A.G.; Bergadà, P.; Vilella, C.; Regué, J.R.; Pijoan, J.; Bardajà, R.; Mauricio, J. A comprehensive sounding of the ionospheric HF radio link from Antarctica to Spain. *Radio Sci.* **2013**, *48*, 1–12. [CrossRef]
13. Pham, C.C.; Nguyen, X.A. Determination of radio wave propagation conditions in the atmosphere of Hanoi using the radiosonde data of balloons. *ICT Express* **2022**, *8*, 611–617. [CrossRef]
14. Teixeira, F.B.; Oliveira, T.; Lopes, M.; Leocádio, C.; Salazar, P.; Ruela, J.; Campos, R.; Ricardo, M. Enabling broadband internet access offshore using tethered balloons: The BLUECOM+ experience. In Proceedings of the IEEE OCEANS 2017, Aberdeen, UK, 19–22 June 2017; pp. 1–7.
15. Stark, J.; McKinney, T.; Booker, Q.; Downey, M.; Golley, E.; Marshall, T.; Roberts, A.; Thompson, J. A Platform for Active Stabilization of High-Altitude Balloon Payloads. *Bull. Am. Meteorol. Soc.* **2023**, *104*, E1132–E1145. [CrossRef]
16. Miś, T.A.; Modelski, J. Risk Assessment and Experimental Light-Balloon Deployment of a Stratospheric Vertical VLF Transmitter. *Sensors* **2023**, *23*, 1073. [CrossRef] [PubMed]
17. McKinney, T.; Perlaky, N.; Danielson, E.; Mohammed, A.; Lee, J.; O'Bryan, B.; Stoll, C.; Hochmuth, C.; Gallien, T.; Kerr, S.; et al. Around the World They Go: Circumnavigating Balloon Satellites! *Bull. Am. Meteorol. Soc.* **2023**, *104*, E192–E207. [CrossRef]
18. Gilfort, J.; Brown, B. WB8ELK: Master of High-Altitude Balloon Projects. *QST Membsh. J. Natl. Assoc. Amat. Radio* **2017** .
19. Brown, B. Wb8ELK SkyTrackers. 2023. Available online: https://gmigliarini.wixsite.com/wb8elk (accessed on 5 February 2023).
20. W5KUB. Amateur Radio Roundtable. 2023. Available online: https://tmedlin.com/ (accessed on 5 February 2023).
21. NIBBB. Northern Illinois Bottlecap Balloon Brigade. 2023. Available online: https://nibbb.org/ (accessed on 5 February 2023).
22. Holmgren, W.F.; Hansen, C.W.; Mikofski, M.A. pvlib python: A python package for modeling solar energy systems. *J. Open Source Softw.* **2018**, *3*, 884. [CrossRef]
23. Electronic. Grey Line HF Radio Propagation. 2021. Available online: https://www.electronics-notes.com/articles/antennas-propagation/ionospheric/greyline-propagation.php (accessed on 5 June 2023).